Hydrol. Earth Syst. Sci. Discuss., 9, 13329–13372, 2012
www.hydrol-earth-syst-sci-discuss.net/9/13329/2012/
doi:10.5194/hessd-9-13329-2012

Hydrology and Earth System Sciences Discussions

Kalman filters for assimilating near-surface observations in the Richards equation – Part 2: A dual filter approach for simultaneous retrieval of states and parameters

H. Medina[1], **N. Romano**[2], **and G. B. Chirico**[2]

[1]Department of Basic Sciences, Agrarian University of Havana, Havana, Cuba
[2]Department of Agricultural Engineering, University of Naples Federico II, Naples, Italy

Received: 3 November 2012 – Accepted: 24 November 2012 – Published: 3 December 2012

Correspondence to: G. B. Chirico (gchirico@unina.it)

Published by Copernicus Publications on behalf of the European Geosciences Union.

Abstract

We present a dual Kalman Filter (KF) approach for retrieving states and parameters controlling soil water dynamics in a homogenous soil column by using near-surface state observations. The dual Kalman filter couples a standard KF algorithm for retrieving the states and an unscented KF algorithm for retrieving the parameters. We examine the performance of the dual Kalman Filter applied to two alternative state-space formulations of the Richards equation, respectively differentiated by the type of variable employed for representing the states: either the soil water content (θ) or the soil matric pressure head (h). We use a synthetic time-series series of true states and noise corrupted observations and a synthetic time-series of meteorological forcing. The performance analyses account for the effect of the input parameters, the observation depth and the assimilation frequency as well as the relationship between the retrieved states and the assimilated variables. We show that the identifiability of the parameters is strongly conditioned by several factors, such as the initial guess of the unknown parameters, the wet or dry range of the retrieved states, the boundary conditions, as well as the form (h-based or θ-based) of the state-space formulation. State identifiability is instead efficient even with a relatively coarse time-resolution of the assimilated observation. The accuracy of the retrieved states exhibits limited sensitivity to the observation depth and the assimilation frequency.

1 Introduction

Retrieving soil water dynamics successfully requires mathematical models that include a proper specification of soil hydraulic parameters as function of variables characterizing the state of the water in the soil (e.g. Heathman et al., 2003; de Lannoy et al., 2007; Vereecken et al., 2008).

Soil water dynamics is commonly modelled with the Richards equation (Richards, 1931), which implements nonlinear relationships between the volumetric soil water

HESSD
9, 13329–13372, 2012

content, θ [$L^3 L^{-3}$], the matric pressure head, h [L], and the hydraulic conductivity, K [$L T^{-1}$], defined by the water retention, $\theta(h)$, and the hydraulic conductivity, $K(\theta)$, functions. However, the assessment of these soil hydraulic functions is subjected to high costs in terms of both labour and time needed for their determination, not only in case of direct measurements but also when indirect methods are applied (Chirico et al., 2007). Particularly for applications over relatively large land areas, significant uncertainties arise from the spatial variability of these hydraulic functions. However, reliable process-based hydrological modelling has highlighted the need to deal with spatial variability issues, as they exert a significant influence on the exchange of water fluxes between the different parts of the system (Chirico et al., 2010). The variability is significant at all scales of interest, making it extremely difficult to capture the hydrological behaviour at one particular scale (Pringle et al., 2007; Nasta et al., 2009). As a result, the parameterization of the soil hydraulic functions is considered one of the main challenges in the current land surface modelling efforts (Zhu and Mohanty, 2004).

The majority of data assimilation studies have focused on retrieving hydrological model states (e.g. soil moisture), while assuming that model parameters are to be specified in advance. There are only few attempts to assimilate near-surface observations for simultaneous retrieval of soil moisture profiles and soil hydraulic parameters.

Common sequential data assimilation methods are based on Kalman filtering, from the pioneering work of Kalman (1960). Although the standard Kalman Filter (SKF) was originally formulated for an optimal recursive solution of linear dynamic models with Gaussian random errors, more recent non-standard Kalman Filters extensions have successfully increased the capabilities to deal with a wider spectrum of nonlinear systems. In particular, those coping with the sequential probabilistic inference problem within nonlinear dynamic systems have experienced considerable progress.

The two most used non-standard Kalman Filters in vadose zone hydrology are the Extended Kalman Filter (EKF) and the Ensemble Kalman Filter (EnKF) (Vereecken et al., 2008). Moradkhani et al. (2005) provided a general framework about the capabilities of a dual EnKF algorithm for streamflow forecasting. Recent studies have been focused

HESSD
9, 13329–13372, 2012

on dual applications using particle filter methods (Qin et al., 2009; Yang et al., 2009; Monztka et al., 2011), another assimilation algorithm that has also gained considerable attention.

The Unscented Kalman Filter (UKF) (Julier et al., 1995; Julier and Uhlman, 1997; van de Merwe, 2004) is a novel, accurate and theoretically well motivated algorithm that has been less applied in hydrological studies. These authors have shown how the UKF consistently outperforms the EKF in terms of estimation accuracy and consistency, at the expenses of the same computational costs. The UKF is based on a deterministic replication of the mean predicted variable for the calculation of the optimal terms in the Gaussian approximate Bayesian update. Gove and Hollinger (2006) applied a dual UKF for the assimilation of net CO2 exchange data in a simple physiological model. Also Tian et al. (2008) used this method for reproducing the temporal evolution of daily soil moisture under freezing conditions by assimilating satellite observations.

Most of the cited dual KF applications have in common the fact that they employ the same KF scheme for sequentially estimating both states and parameters (e.g. EKF, UKF, etc.).

Chirico et al. (2012) showed that state retrieval can take advantage from a finite differentiation of the Richards equation based on the Crank-Nicolson linear numerical scheme, which can be coupled with a standard KF (SKF) algorithm much more efficiently than a non-linear numerical scheme coupled with a non-standard KF algorithm. The study also showed that UKF is more efficient than EKF when one has to deal with the typical nonlinearity of the soil hydraulic property functions. Therefore, the present study suggests dual Kalman Filter approach combining a SKF for an optimal retrieval of the states, while limiting the application of an approximate UKF only for the sequential update of the parameters characterizing the soil hydraulic properties.

The first objective of this study is to illustrate the performance of the dual Kalman Filter approach based on the standard retrieving of the states and the unscented retrieving of soil hydraulic parameters, by assimilating near-surface soil moisture information in a one-dimensional Richards' equation using synthetic data. A second objective is to

HESSD
9, 13329–13372, 2012

comparatively assess the potential advantageous and limitations attached to the implementation of an h-based or a θ-based form of the Richards equation in the retrieving algorithm, according to different initial guess of the parameters, observation depths, assimilation frequencies as well as the type of near-surface observations (h or θ).

2 Methods

2.1 The dual Kalman filter formulation

The dual KF equations are the result of a concatenation of the state and parameter KF equations. Both hidden system states $\boldsymbol{x}_k$, and model parameters $\boldsymbol{w}_k$, with initial probability density $p(\boldsymbol{x}_k)$ and $p(\boldsymbol{w}_k)$, respectively, evolve over time t_k according to the conditional probability density $p(\boldsymbol{x}_k|\boldsymbol{x}_{k-1})$ and $p(\boldsymbol{w}_k|\boldsymbol{w}_{k-1})$. The observations $\boldsymbol{y}_k$, responding to the conditional probability density $p(\boldsymbol{y}_k|\boldsymbol{x}_k, \boldsymbol{w}_k)$, serve to the simultaneous estimation of $\boldsymbol{x}$ and $\boldsymbol{w}$. A separate state-space representation is used for the signal and the weights. At every time step, the current estimate of the weights is used in the signal-filter, and the current estimate of the signal-state is used in the weight-filter.

The set of system equations for states can be written as:

$$\boldsymbol{x}_k = F\left(\boldsymbol{x}_{k-1}, \boldsymbol{u}_{k-1}, \boldsymbol{v}_{k-1}, \hat{\boldsymbol{w}}_{k-1}\right) \quad (1)$$

$$\boldsymbol{y}_k = H\left(\boldsymbol{x}_k, \boldsymbol{n}_k, \hat{\boldsymbol{w}}_{k-1}\right). \quad (2)$$

The set of system equations for parameters can be written as:

$$\boldsymbol{w}_k = \boldsymbol{w}_{k-1} + \boldsymbol{r}_{k-1} \quad (3)$$

$$\boldsymbol{y}_k = H\left(F\left(\hat{\boldsymbol{x}}_{k-1}, \boldsymbol{u}_{k-1}, \boldsymbol{v}_{k-1}, \boldsymbol{w}_{k-1}\right), \boldsymbol{n}_k, \boldsymbol{w}_k\right). \quad (4)$$

In the equation above, $\boldsymbol{u}_k$ is the exogenous input assumed known, $\boldsymbol{v}_k$ is the process noise that drives the dynamic system through the state transition function F, and $\boldsymbol{n}_k$ is the observation or measurement noise corrupting the observation of the state through the observation function H. The main problem of a non-standard Kalman filter is to

HESSD
9, 13329–13372, 2012

calculate the expected mean and variance of a random variable under nonlinear F and/or H transformations.

The state transition density $p(\boldsymbol{x}_k|\boldsymbol{x}_{k-1})$ is fully specified by F and the process noise distribution $p(\boldsymbol{v}_k)$, whereas H and the observation noise distribution $p(\boldsymbol{n}_k)$ fully specify the observation likelihood $p(\boldsymbol{y}_k|\boldsymbol{x}_k, \boldsymbol{w}_k)$. Both F and/or H are parameterized via the parameter vector $\boldsymbol{w}_k$, corresponding to a stationary process with identity state transition matrix, driven by process noise $\boldsymbol{r}_k$. The upper symbol "" denotes the posterior density mean of the variable.

Using a generic symbol $\boldsymbol{z}_k$ for referring to both states, $\boldsymbol{x}_k$, and parameters, $\boldsymbol{w}_k$, the posterior density mean and covariance of these variables, $\hat{\boldsymbol{z}}_k$ and $\mathbf{P}_{z_k}$, respectively, can be calculated according to the Kalman approach as:

$$\hat{\boldsymbol{z}}_k = \left(\text{prediction of } \hat{\boldsymbol{z}}_k\right) + \mathbf{K}_k^z \left(\boldsymbol{y}_k - \left(\text{prediction of } \boldsymbol{y}_k\right)\right) = \left(\hat{\boldsymbol{z}}_k^-\right) + \mathbf{K}_k^z \left(\boldsymbol{y}_k - \hat{\boldsymbol{y}}_k^-\right) \tag{5}$$

$$\mathbf{P}_{z_k} = \mathbf{P}_{z_k}^- - \mathbf{K}_k^z \mathbf{P}_{y_k}^z \left(\mathbf{K}_k^z\right)^T \tag{6}$$

where the Kalman gain $\mathbf{K}_k^z$ is calculated according to:

$$\mathbf{K}_k^z = \mathbf{P}_{z_k y_k} \left(\mathbf{P}_{\tilde{y}_k}^z\right)^{-1}. \tag{7}$$

The variables $\hat{\boldsymbol{z}}_k^-$ and $\mathbf{P}_{z_k}^-$ represents the optimal prediction (prior mean at time t_k) of $\boldsymbol{z}_k$ and $\mathbf{P}_{z_k}$. The optimal gain term $\mathbf{K}_k^z$ is expressed as a function of the expected cross-covariance matrix of the process prediction error and the observation prediction error, $\mathbf{P}_{z_k y_k}$, and the expected auto-covariance matrix of the observation prediction error, $\mathbf{P}_{\tilde{y}_k}^z$.

2.1.1 SKF algorithm for state retrieval

The standard algorithm for the states retrieving is structured according to the following three steps.

HESSD
9, 13329–13372, 2012

Initialization:

$$\hat{\boldsymbol{x}}_0 = E\left[\boldsymbol{x}_0\right] \tag{8}$$

$$\mathbf{P}_{x_0} = E\left[\left(\boldsymbol{x}_0 - \hat{\boldsymbol{x}}_0\right)\left(\boldsymbol{x}_0 - \hat{\boldsymbol{x}}_0\right)^T\right] \tag{9}$$

$$\mathbf{R}_{v_0} = E\left[\left(\boldsymbol{v}_0 - \overline{\boldsymbol{v}}_0\right)\left(\boldsymbol{v}_0 - \overline{\boldsymbol{v}}_0\right)^T\right] \tag{10}$$

$$\mathbf{R}_{n_0} = E\left[\left(\boldsymbol{n}_0 - \overline{\boldsymbol{n}}_0\right)\left(\boldsymbol{n}_0 - \overline{\boldsymbol{n}}_0\right)^T\right] \tag{11}$$

where $\mathbf{R}_v$ denotes the auto covariance matrix of the process noise, while $\mathbf{R}_n$ the auto covariance matrix of the observation noise.

Prediction step by computing the state mean and covariance, within each time-step k:

$$\hat{\boldsymbol{x}}_k^- = F\left(\hat{\boldsymbol{x}}_{k-1}, \boldsymbol{u}_{k-1}, \boldsymbol{v}_{k-1}, \hat{\boldsymbol{w}}_{k-1}\right) \tag{12}$$

$$\mathbf{P}_{x_k}^- = \mathbf{F}\mathbf{P}_{x_{k-1}}\mathbf{F}^T + \mathbf{F}\mathbf{R}_v\mathbf{F}^T \tag{13}$$

where $\mathbf{R}_v$ is the auto covariance matrix of the process noise, and the model operator F in Eq. (12) is linear and thus is represented by the matrix $\mathbf{F}$.

Correction step for updating estimates with the last observation:

$$\mathbf{K}_k^x = \mathbf{P}_{x_k}^- \mathbf{H}_{x_k}^T \left(\mathbf{H}_{x_k}\mathbf{P}_{x_k}^- \mathbf{H}_{x_k}^T + \mathbf{H}_{x_k}\mathbf{R}_n\mathbf{H}_{x_k}^T\right)^{-1} \tag{14}$$

$$\hat{\boldsymbol{x}}_k = \left(\hat{\boldsymbol{x}}_k^-\right) + \mathbf{K}_k\left(\boldsymbol{y}_k - \mathbf{H}\left(\hat{\boldsymbol{x}}_k^-, \boldsymbol{n}\right)\right). \tag{15}$$

Equations (14) and (15) assume that measurement operator H in Eq. (2) is linear and thus is represented by the matrix $\mathbf{H}$. The linearity or nonlinearity is conditioned in principle to the relationship between the type of assimilated data and the form of the state equation, as discussed later in this paper. For a nonlinear H, a non-standard KF extension would be necessary.

HESSD
9, 13329–13372, 2012

2.1.2 UKF algorithm for parameter retrieval

From an optimization perspective, the Kalman filter parameter estimation looks for minimizing the following prediction-error cost:

$$J = \sum_{t=1}^{k} \left(\boldsymbol{y}_t - \hat{\boldsymbol{y}}_t^-\right)^T \left(\mathbf{R}_{e_t}\right)^{-1} \left(\boldsymbol{y}_t - \hat{\boldsymbol{y}}_t^-\right) \tag{16}$$

where $\mathbf{R}_e$ an artificial noise parameter covariance.

In the UKF, the distribution of the parameters, as in the more known Extended Kalman Filter, is still represented by a Gaussian random variable, but it is specified by a minimal set of deterministically chosen sample points. Sample points selection strategy is finalized to capture the true mean and covariance of the variable and, after being propagated through the true nonlinear system, to capture the posterior mean and covariance with a second order accuracy for any nonlinearity, with errors only introduced in the third and higher orders.

Considering $\overline{\boldsymbol{w}}$ and $\mathbf{P}_w$ as mean and covariance, respectively, of the parameter vector $\boldsymbol{w}$ to be retrieved, having dimension L, the UKF, in the simpler mode, obtains a set of $2L+1$ points, named sigma points, $\mathbf{S}_i = \{\mu_i, \boldsymbol{W}_i,\ i = 1 \ldots L\}$, completely capturing the actual mean and covariance of the prior random variable $\boldsymbol{w}$. A selection of sigma points fulfilling this requirement is defined as follows:

$$\begin{aligned}
&\boldsymbol{W}_0 = \overline{\boldsymbol{w}} && \mu_0^{(m)} = \tfrac{\gamma - L}{\gamma} \\
&\boldsymbol{W}_i = \overline{\boldsymbol{w}} + \left(\sqrt{\gamma \mathbf{P}_w}\right)_i \quad i = 1, \ldots, L && \mu_0^{(c)} = \tfrac{\gamma - L}{\gamma} + \left(1 - \rho^2 + \beta\right) \\
&\boldsymbol{W}_i = \overline{\boldsymbol{w}} - \left(\sqrt{\gamma \mathbf{P}_w}\right)_i \quad i = L+1, \ldots, 2L && \mu_i^{(m)} = \mu_i^{(c)} = \tfrac{1}{2(\gamma)} \qquad i = 1, \ldots, 2L
\end{aligned} \tag{17}$$

where μ_i are the weights related to the point i, conditioned to $\sum_{i=0}^{2L} \mu_i = 1$. Weight values for calculating the mean and the covariance are distinguished by the upper indexes

HESSD
9, 13329–13372, 2012

m and c, respectively. The other parameters are defined as follows: $\gamma = \rho^2(L + \kappa)$, being ρa factor allowing to expand or to shrink the sigma point distribution around the mean; κ is a scaling parameter; β affects the weights of the points when calculating the covariance. Details about the proper choice of ρ, β and κcan be found in the work of van der Merwe (2004). The term $\left(\sqrt{\gamma \mathbf{P}_w}\right)_i$ is the i-th column (or row) of the root square matrix $\gamma \mathbf{P}_w$, calculated by Cholesky decomposition (Press et al., 1992).

Given the above sampling strategy, the algorithm for retrieving the dynamic parameter is structured according to the following four steps.

Initialization

$$\hat{\boldsymbol{w}}_0 = E[\boldsymbol{w}] \tag{18}$$

$$\mathbf{P}_{w_0} = E\left[\left(\boldsymbol{w} - \hat{\boldsymbol{w}}_0\right)\left(\boldsymbol{w} - \hat{\boldsymbol{w}}_0\right)^T\right]. \tag{19}$$

Time update equations, within each time-step k

$$\hat{\boldsymbol{w}}_k^- = \hat{\boldsymbol{w}}_{k-1} \tag{20}$$

$$\mathbf{P}_{w_k}^- = \mathbf{P}_{w_{k-1}} + \mathbf{R}_{r_{k-1}} \tag{21}$$

where $\mathbf{R}_r$ is the artificial innovation covariance.

Calculate the sigma points for the measuring update according to:

$$\boldsymbol{W}_{k-1} = \left[\hat{\boldsymbol{w}}_{k-1} \quad \hat{\boldsymbol{w}}_{k-1} + \sqrt{\gamma \mathbf{P}_{k-1}} \quad \hat{\boldsymbol{w}}_{k-1} - \sqrt{\gamma \mathbf{P}_{k-1}}\right]. \tag{22}$$

Measuring update equations

$$\boldsymbol{Y}_{k|k-1} = H\left(F\left(\hat{\boldsymbol{x}}_{k-1}, \boldsymbol{u}_{k-1}, \boldsymbol{v}_{k-1}, \boldsymbol{W}_{k-1}\right)\right). \tag{23}$$

HESSD
9, 13329–13372, 2012

The output function is obtained as:

$$\hat{\boldsymbol{y}}_{w_k}^{-} = \sum_{i=0}^{2L_w} \mu_i^{(m)} \boldsymbol{Y}_{i,k|k-1}^{z} \tag{24}$$

$$\mathbf{P}_{w_k y_k} = \sum_{i=0}^{2L} \mu_i^{(c)} \left(\boldsymbol{W}_{i,k|k-1} - \hat{\boldsymbol{w}}_k^{-}\right) \left(\boldsymbol{Y}_{i,k|k-1} - \hat{\boldsymbol{y}}_k^{-}\right)^T \tag{25}$$

$$\mathbf{P}_{\tilde{y}_k} = \sum_{i=0}^{2L} \mu_i^{(c)} \left(\boldsymbol{Y}_{i,k|k-1} - \hat{\boldsymbol{y}}_k^{-}\right) \left(\boldsymbol{Y}_{i,k|k-1} - \hat{\boldsymbol{y}}_k^{-}\right)^T + \mathbf{R}_{e_k} \tag{26}$$

$$\mathbf{K}_k^w = \mathbf{P}_{w_k y_k} \mathbf{P}_{\tilde{y}_k}^{-1} \tag{27}$$

$$\hat{\boldsymbol{w}}_k = \hat{\boldsymbol{w}}_{k-1}^{-} + \mathbf{K}_k^w \left(\boldsymbol{y}_k - \hat{\boldsymbol{y}}_k^{-}\right) \tag{28}$$

$$\mathbf{P}_{w_k} = \mathbf{P}_{w_k}^{-} - \mathbf{K}_k^w \mathbf{P}_{\tilde{y}_k}^w \left(\mathbf{K}_k^w\right)^T. \tag{29}$$

Van der Merwe (2000) suggested several options on how to choose the matrix $\mathbf{R}_r$.

$\mathbf{R}_r$ as an arbitrary "fixed" diagonal value, which may then be annealed toward zero as training continues;

$$\mathbf{R}_{r_k} = \left(\lambda_{\mathrm{RLS}}^{-1} - 1\right) P_{w_k} \tag{30}$$

where $\lambda_{\mathrm{RLS}} \in (0, 1]$ is considered a forgetting factor as defined in the recursive least-squares (RLS) algorithm (Nelson, 2000). This provides for an approximate exponentially decaying weighting on past data;

$$\mathbf{R}_{r_k} = (1 - \alpha_{\mathrm{RM}}) \mathbf{R}_{r_{k-1}} + \alpha_{\mathrm{RM}} \mathbf{K}_k^W \left[\boldsymbol{y}_k - H\left(\boldsymbol{x}_k, \hat{\boldsymbol{x}}_k^{-}\right)\right] \left[\boldsymbol{y}_k - H\left(\boldsymbol{x}_k, \hat{\boldsymbol{x}}_k^{-}\right)\right]^T \left(\mathbf{K}_k^W\right)^T \tag{31}$$

which is a Robbins-Monro stochastic approximation scheme for estimating the innovations, where $\alpha_{\mathrm{RM}} \in (0, 1]$.

HESSD
9, 13329–13372, 2012

Typically, $\mathbf{R}_r$ is also constrained to be a diagonal matrix, which implies an independence assumption on the parameters.

$\mathbf{R}_e$ in Eq. (26) is commonly assumed as a constant diagonal matrix, although in principle some adaptive strategies can be also used (Wan and Nelson, 1997; van der Merwe, 2004). The effect produced by the parameter covariances on convergence rate and parameter tracking performance is discussed later in the study.

3 Application to one-dimensional Richards' equation

3.1 Governing equation

As in the vast majority of applications in this realm, we describe the vertical movement of water under isothermal conditions in a rigid, homogeneous, variably saturated porous medium using the Richards equation (Jury et al., 1991). The following two equations represent the Richards equation in the h-based and in θ-based forms, respectively:

$$\frac{\partial \theta}{\partial t} = C(h)\frac{\partial h}{\partial t} = \frac{\partial \left[K(h)\left(\frac{\partial h}{\partial z} - 1\right)\right]}{\partial z} \tag{32}$$

$$\frac{\partial \theta}{\partial t} = \frac{\partial \left[D(\theta)\frac{\partial \theta}{\partial z} - K(\theta)\right]}{\partial z} \tag{33}$$

where t is time and z is soil depth taken positive downward with $z = 0$ at the top of the profile, $C(h) = \partial\theta/\partial h$ [1/L] represents the specific water capacity of the soil at pressure head h obtained by differentiating $\theta(h)$, and $D(\theta) = K(\theta)/C(\theta)$ [$\mathrm{L}^2\,\mathrm{T}^{-1}$] represents the unsaturated diffusivity.

For an efficient numerical solution of the model, it is convenient to describe the soil hydraulic properties using closed-form analytical relationships. The following non-hysteretic van Genuchten-Mualem (VGM) relations (van Genuchten, 1980) are widely used in soil hydrology:

HESSD
9, 13329–13372, 2012

$$\theta(h) = \theta_r + \theta_s - \theta_r \left[1 + |\alpha h|^n\right]^{-m} \tag{34}$$

$$K(\theta) = K_s S_e^{\lambda} \left[1 - \left(1 - S_e^{1/m}\right)^m\right]^2 \tag{35}$$

where θ_s is the saturated soil water content, θ_r is the residual soil water content, $S_e = (\theta - \theta_r)/(\theta_s - \theta_r)$ is the effective saturation, K_s is the saturated hydraulic conductivity and α [L^{-1}], n (–), m (–) and λ (–) are empirical scale and shape parameters. A common assumption, also adopted in this work, is to fix $\lambda = 0.5$ and pose $m = 1 - 1/n$.

3.2 Crank-Nicolson finite difference scheme (CN)

Chirico et al. (2012) showed that the efficiency of a KF-based algorithm in retrieving states by assimilating near surface observations is strictly linked to the numerical scheme employed for differentiating the Richards equation and implemented in the dynamic state-space model. According to this study, a standard KF applied upon a linearized Crank-Nicolson (CN) scheme of the Richards equation results more efficient than an UKF approach under a nonlinear backward Euler algorithm. For intermediate nodes, the differentiation of Eq. (31) according to the CN scheme leads to the expression:

$$\begin{pmatrix} -\dfrac{K_{i-1/2}^k}{2\Delta z_i \Delta z_u}; & \dfrac{C_i^k}{\Delta t^k} + \dfrac{\frac{K_{i-1/2}^k}{\Delta z_u} + \frac{K_{i+1/2}^k}{\Delta z_l}}{2\Delta z_i}; & -\dfrac{K_{i+1/2}^k}{2\Delta z_i \Delta z_l} \end{pmatrix} \begin{pmatrix} h_{i-1}^{k+1} \\ h_i^{k+1} \\ h_{i+1}^{k+1} \end{pmatrix}$$

$$= \begin{pmatrix} \dfrac{K_{i-1/2}^k}{2\Delta z_i \Delta z_u}; & \dfrac{C_i^k}{\Delta t^j} - \dfrac{\frac{K_{i-1/2}^k}{\Delta z_u} + \frac{K_{i+1/2}^k}{\Delta z_l}}{2\Delta z_i}; & \dfrac{K_{i+1/2}^k}{2\Delta z_i \Delta z_l} \end{pmatrix} \begin{pmatrix} h_{i-1}^k \\ h_i^k \\ h_{i+1}^k \end{pmatrix} + \frac{K_{i-1}^k - K_{i+1}^k}{2\Delta z_i} \tag{36}$$

HESSD
9, 13329–13372, 2012

where subscript i is the node number (increasing downward), superscript k is the time level, and $\Delta t^k = t^{k+1} - t^k$. All nodes, including the top and bottom node, are in the centre of the soil compartments, with $\Delta z_u = z_i - z_{i-1}$, $\Delta z_l = z_{i+1} - z_i$ and Δz_i the compartment thickness. The spatial averages of K are calculated as arithmetic means.

Assuming flux boundary conditions, the differential equations at the top and bottom nodes respectively are:

$$\left(\frac{C_1^k}{\Delta t^j} + \frac{K_{1+1/2}^k}{2\Delta z_1 \Delta z_l};\ -\frac{K_{1+1/2}^k}{2\Delta z_1 \Delta z_l}\right)\begin{pmatrix} h_1^{k+1} \\ h_2^{k+1} \end{pmatrix} = \left(\frac{C_1^k}{\Delta t^k} - \frac{K_{1+1/2}^k}{2\Delta z_1 \Delta z_l};\ \frac{K_{1+1/2}^k}{2\Delta z_1 \Delta z_l}\right)\begin{pmatrix} h_1^k \\ h_2^k \end{pmatrix} + \frac{Q_{\text{top}} - K_{1+1/2}^k}{\Delta z_1} \tag{37}$$

$$\left(-\frac{K_{n-1/2}^k}{2\Delta z_n \Delta z_u};\ \frac{C_n^k}{\Delta t^k} + \frac{K_{n-1/2}^k}{2\Delta z_n \Delta z_u}\right)\begin{pmatrix} h_{n-1}^{k+1} \\ h_n^{k+1} \end{pmatrix} = \left(\frac{K_{n-1/2}^k}{2\Delta z_n \Delta z_u};\ \frac{C_n^k}{\Delta t^k} - \frac{K_{n-1/2}^k}{2\Delta z_n \Delta z_u}\right)\begin{pmatrix} h_{n-1}^k \\ h_n^k \end{pmatrix} + \frac{K_{n-1/2}^k - Q_{\text{bot}}}{\Delta z_n} \tag{38}$$

being Q_{top} and Q_{bot} the flux at the top and the bottom of the soil profile.

The analogous differential expressions of the Richards equation in the θ-form (Eq. 33) can be obtained from Eqs. (36)–(38) by simply removing the soil water capacity (C) and by substituting h with θ, the hydraulic conductivity (K) of the dependent terms with the diffusivity (D), while keeping intact the independent terms on the right-hand side.

Notice that these equations can be conveniently written in state-space representation as:

$$\mathbf{A}_{k+1}\,\boldsymbol{x}_{k+1} = \mathbf{A}'_k\,\boldsymbol{x}_k + \boldsymbol{f}_k \tag{39}$$

HESSD
9, 13329–13372, 2012

where $\boldsymbol{x}$ represents the state vector, either soil moisture or pressure heads in the soil profile, while $\mathbf{A}$ and $\mathbf{A}'$ are tri-diagonal matrices and $\boldsymbol{f}$ a vector of size n. Hence, its solution does not require a recursive calculation, but it involves the inversion of matrix $\mathbf{A}$. More explicitly Eq. (37) becomes:

$$\boldsymbol{x}_{k+1} = \mathbf{B}_k \boldsymbol{x}_k + \boldsymbol{g}_k \tag{40}$$

by making $\mathbf{B} = \mathbf{A}^{-1}\mathbf{A}'$ and $\boldsymbol{g} = \mathbf{A}^{-1}\boldsymbol{f}$.

3.3 Algorithm implementation for state and parameter retrievals

The synthetic study examines the possibility to retrieve either pressure head or soil water content as state variable, changing also the type of observed variable with respect to that retrieved.

The retrieved parameters are only the parameters of the van Genuchten analytical model: K_s, α, and n. We assume parameters θ_s and θ_r to be known, as they can be determined with more ease.

Given the marked differences in the range of variation of the VGM parameters, a variable transformation is required to guarantee operational stability. Bounding parameters by means of a function of reference values and a variable correction term, ensure a reliable behaviour of the model. Considering that w_i is the true value of the i-th parameter, the parameter estimation system makes use of the following variable transformation:

$$w_i = w_{i_{\min}} + \left(w_{i_{\max}} - w_{i_{\min}}\right) \boldsymbol{g}(\delta w_i) \tag{41}$$

where $w_{\min}$ and $w_{\max}$ represent user-defined nominal values, defining the minimum and the maximum values of the parameter, respectively, while the correction term δw, to be actually the variable under estimation, is expressed as independent terms of one nonlinear sigmoidal function $\boldsymbol{g}(\delta w)$. This function $\boldsymbol{g}(\delta w)$, defined "squashing function" by van der Merwe (2004), limits the absolute magnitude of the iterative parameter adjustment, further preventing the divergence of the parameter estimations. Therefore, the parameters are not estimated directly, rather "correction terms" are estimated.

HESSD
9, 13329–13372, 2012

A preliminary analysis has shown that the approach is not very sensitive to the type of sigmoidal function and that the following relationship performed well for all of the circumstances examined:

$$\boldsymbol{g}(\delta w_i) = \frac{\delta w_i}{2(1 + |\delta w_i|)} + 0.5. \quad (42)$$

Notice that $\lim_{\delta w_i \to -\infty} g(\delta w_i) = 0$ and $\lim_{\delta w_i \to \infty} g(\delta w_i) = 1$, in which case, $w_i = w_{i_{\min}}$ and $w_i = w_{i_{\max}}$, respectively.

4 Synthetic experimental framework

We explore the performance of the proposed dual Kalman Filter with a synthetic study. The main advantage of testing the algorithm with a synthetic study is the fact that by knowing the true system, the results are not overshadowed by other sources of uncertainty: a fundamental aspect that is important to address prior evaluating the algorithm performance with real data, as presented in Medina et al. (2012).

The synthetic study involves the retrieval of states and parameters by assimilating near-surface observations into the Richards equation, according to three different retrieving modes (RM):

- the $h - h$ retrieving mode, indicating that pressure heads are used both as observed variables and state variables, with the h-based form of the Richards equation;
- the $\theta - \theta$ retrieving mode, indicating that soil moisture contents are used both as observed variables and state variables, with the θ-based form of the Richards equation;
- the $\theta - h$retrieving mode, indicating that soil moisture contents are used as the observed variable while pressure heads are used as state variables, with the h-based form of the Richards equation.

HESSD
9, 13329–13372, 2012

We evaluate the performance of the dual KF approach by comparing the retrieved variables with their synthetic "true" counterparts, which are obtained by means of a simple model realization with known initial state and input parameters. The observations being assimilated are the actual synthetic model realization plus a white noise.

The hydraulic properties of the uniform soil column are identified by using the VGM parameters reported in the papers by Entekhabi et al. (1994) and Walker et al. (2001): $\theta_{s_T} = 0.54$; $\theta_{r_T} = 0.2$; $K_{s_T} = 0.00029\,\mathrm{cm\,s^{-1}}$, $\alpha_T = 0.008\,\mathrm{cm^{-1}}$ and $n_T = 1.8$, where the subscript T indicates the "true" values, i.e. those employed for the synthetic model realization. However, different boundary conditions have been set so as to make the synthetic study more representative from a practical perspective:

- the top boundary condition is the result of a combination of a stochastically generated daily series plus a constant evaporation rate of $2.35\,\mathrm{mm\,day^{-1}}$;
- the bottom boundary condition is set by a zero gradient of the soil water pressure head, also known as "free drainage" condition, which also implies that this condition is affected by the uncertainty attached to hydraulic conductivity.

The inclusion of a rainfall pattern allows for evaluating the dual filter performance during continuous wetting and drying processes taking place in the soil profile. In mathematical terms, it also reduces the state correlations along the profile, thus making the synthetic study a more representative stress test of the overall retrieving process as compared with a constant top boundary condition as in Entekhabi et al. (1994) and Walker et al. (2001).

Daily rainfall is obtained by stochastically sampling a Poisson probability distribution of the occurrence of daily events with an exponential distribution of the rainfall depth. The bar plot in Fig. 1 illustrates the synthetic daily rainfall time-series for a period of 150 days.

Subsequently, time series of soil water pressure head and soil moisture profiles are generated for 150 days taking a uniform −50 cm pressure head profile as initial condition. To improve the efficiency of the numerical scheme with respect to the local

HESSD
9, 13329–13372, 2012

state gradients, we have adopted a heterogeneous discretisation involving 27 nodes, in a way different from the uniform partition employed by Entekhabi et al. (1994) and Walker et al. (2001). Figure 1 also shows the time series of the generated pressure head values at 5 cm depth.

We simulate the assimilation of observed variables at three alternative observation depths (OD): 2, 5 and 10 cm. Escorihuela et al. (2010) found 2 cm as the most effective soil moisture sampling depth by the L-band radiometry. Nevertheless, L-band sensors receive their signal from approximately the top 5 cm, on average (Kerr, 2007). A depth of 10 cm represents the maximum observation depth that can be likely explored with the current technology (Walker, 1999).

We also examine three alternative assimilation frequencies (AF): 1, 1/3 and 1/5 days^{-1}. Daily assimilation frequency accounts for future L-band missions or to a combination of different sensors, whilst 3 days is the minimum time-interval of SMOS spaceborne platforms (Montzka et al., 2001). One observation every 5 days represents a more common remote sensing time frequency. Table 1 summarizes the values of the main parameters and initial conditions taking part in the retrieving algorithms herein applied.

The initial soil moisture profile for the θ-based retrieving algorithm is derived by applying the VGM water retention relation to the initial pressure head profile chosen for the h-based retrieving algorithm. A similar approach has been adopted for setting the initial state covariance in the θ-based form.

The initial covariance matrices are considered diagonal for all cases. The initial state covariance matrix in h-form is defined as 10^3 cm^2 on the diagonal elements (ten times the initial state), representing a sufficiently high error in the initial pressure head profile with no correlation between nodes. The initial matrix of the normalized correction terms associated to the soil hydraulic parameters is set to 0.01 on the diagonal elements, following Nelson (2000).

The observation noise variance is updated as a diagonal matrix and set equal to 2 % of the absolute observed state vector, following Entekhabi et al. (1994) and Walker et

HESSD
9, 13329–13372, 2012

al. (2001). Similarly, the system noise covariance is set to 5 % of the profile state vector, as also done by Entekhabi et al. (1994). For this variable, Walker et al. (2001) opted for a more conservative 5 % of the change in the system state vector.

We also considered six very dissimilar sets of initial values for the parameters K_s, α, and n so as to evaluate the role exerted by different initial guesses on the performance of the retrieving process. These initial values have been identified by employing the six possible permutations of the values −1, 0 and 1 as correction terms δw_i in Eq. (40), and subsequently in Eq. (39). Table 2 shows the resulting initial values of the parameters and the corresponding $w_{\min}$ and $w_{max} - w_{\min}$.

For quantitatively evaluating the performance of the retrieving algorithms, the normalized mean error (ME) and the root mean square (RMSE) between predicted and synthetic data (SD) state profiles are calculated as follows:

$$\mathrm{ME}_j = \frac{1}{\sigma_{\mathrm{SD}}} \left[\sum_{i=1}^{N_{\mathrm{nod}}} \left(x_{i,j}^{\mathrm{p}} - x_{i,j}^{\mathrm{SD}} \right) / N_{\mathrm{nod}} \right] \tag{43}$$

$$\mathrm{RMSE}_j = \sqrt{\frac{1}{\sigma_{\mathrm{SD}}} \left[\sum_{i=1}^{N_{\mathrm{nod}}} \left(x_{i,j}^{\mathrm{p}} - x_{i,j}^{\mathrm{SD}} \right)^2 / (N_{\mathrm{nod}} - 1) \right]} \tag{44}$$

where $x_{i,j}^{p}$ and $x_{i,j}^{\mathrm{SD}}$ represent the predicted and SD state value at node i and time j, respectively, and σ_{SD} is the standard deviation of the SD state series. The normalization is carried out for enabling the comparisons between θ-based and h-based retrieving processes.

HESSD
9, 13329–13372, 2012

5 Results

5.1 Stability of the retrieving algorithms

As part of this synthetic study, we evaluate the retrieving algorithm when alternatively using the h-based or the θ-based form of the Richards equation. An important aspect, also addressed by Walker et al. (2001), concerns the stability issues attached to these two alternative formulations. A first problem, encountered when retrieving the pressure heads, is a failure of the algorithms due to relatively abrupt changes in the state variable. To cope with this problem, we apply a log-transformation to the pressure head values, thus reducing the relative differences between near-surface observations and model predictions. Nonetheless, despite this variable log-transformation, several retrieving exercises still failed, in particular when sharp pressure gradients are established after approximately 110 days of simulation. This failure is more frequent when near-surface observations are assimilated every day than every three or five days. In fact, the probability of abrupt state changes increases as the observation frequency increases.

Another important factor yielding possible failures is the irreversible deformation of the correlation structure between parameters, when parameter updates sample limit values of the corresponding admissible ranges. Notice that the derivative of the sigmoidal function used in the parameter transformation (Eq. 42) tends to zero when the independent variable tends to ∞ and $-\infty$. In practical terms, it means that the sigmoidal function becomes insensible to further updates and therefore can diverge. This issue, more frequently found with larger time intervals between the assimilated observations, is in turn connected to certain parameter initialization as shown later.

In the h-based form, difficulties have been found in tuning the covariance matrices in order to get a considerable number of safe simulations for the entire period of 150 days. The variation of the initialisation conditions, including the initial parameter values, usually demands to retouch the parameter covariance matrices for sake of stability. However, provided that the algorithm is stable, the results are not particularly sensitive to

HESSD
9, 13329–13372, 2012

the actual chosen covariance values. The specific role of these covariance matrices is also illustrated later.

On the contrary, the retrieving algorithm using soil moisture as state variable is permanently stable. As stated by Walker et al. (2001), the soil moisture transformation not only reduces the differences between model predictions and observations, but also smoothes the nonlinearities along the soil profile. Parameter covariance matrices do not need to be adjusted when initialisation values are changed. These results are perceived as a significant advantage of the θ-form as compared with the h-form.

5.2 Parameter identifiability

Figure 2 illustrates the retrieved parameters Ks, α and n from daily assimilations using both, the h – h and θ-form retrieving modes. These graphs depict the evolving patterns with the three alternative observation depths (OD = 2, 5 and 10 cm).

The "true" value of α is rapidly identified during the retrieving process, independently from the retrieving mode. Parameter α is also the least affected by the initial guess of the parameters under scrutiny, especially when using pressure heads as state variables. Indeed, parameter α acts as a scaling factor of the state values in the soil hydraulic property functions, thus its retrieval is highly sensitive to the convergence rate of the first moment of the state vector. Vrugt et al. (2001, 2002) found that most of the information on α is embedded in soil water content observations just beyond the air entry value of the soil. Accordingly, in the present study, the identifiability of α is probably favoured by the relatively wet states explored in the initial stage of the synthetic experiment.

The identifiability of parameter α is seemingly also related to the relative position of the observations in the soil profile, depending on the type of simulated process. Ritter et al. (2004) performed a sensitivity analysis of three state variables (soil moisture, pressure head and bottom flux) to the VGM parameters using a soil profile with four soil horizons and found that the average sensitivity of α was higher than that of n by about a factor of 2, particularly for the uppermost horizon. For the deeper horizons,

HESSD
9, 13329–13372, 2012

instead, the sensitivity to n was almost three times higher. This is an interesting aspect, particularly for the issues related to near-surface observations.

Persistent failures occur when taking the initial parameter set S3 with all three observation depths, and when taking S6 with 5 and 10 cm observation depths, as shown by the anomalous or truncated evolving values. These failures are associated to a relatively abrupt decrease in pressure heads after about 110 days from the start of the simulation runs.

It is important to keep in mind the sequential and Bayesian nature of the dual filter approach, together with the limited variability of the successive surface observations being assimilated. Several authors evidenced the limitations for a successful estimation of VGM parameters, as imposed by the narrow variability of naturally occurring boundary conditions (Scharnagl et al., 2011; Vrugt et al., 2001, 2002). A wide range of soil moisture states in required to reliably constraining the soil hydraulic functions.

Unlike parameter α, the saturated hydraulic conductivity, K_s, is identified with much more difficulty. This can be due in part to the fact that the water retention parameters also feature in the hydraulic conductivity function, thus enhancing the occurrence of high correlations among the model parameters. A strong correlation is found between retrieved parameters n and Ks. It is known that this strong interdependence also affects the performance of the VGM model. Especially for certain soil types, Romano and Santini (1999) showed that decoupling the hydraulic conductivity function from the water retention function can lead to more successful inverse modelling results. As a strategy to reduce the relative uncertainty, Scharnagl et al. (2011) suggested that the parameter K_s should be assessed soon after the rainfall events, when soil moisture redistributes more rapidly in the entire soil profile, being essentially driven by gravity.

The convergence and tracking process of n depend more upon the assimilation mode. In the h-form, sensible differences can be observed between the evolving patterns whether one assumes $n < 2$ or $n > 2$ as initial guess. The convergence toward the true n is more delayed as compared with α. In some cases, convergence fails for $n > 2$, particularly for $n = 2.6$, which is the highest initial guess value explored in this study.

HESSD
9, 13329–13372, 2012

This situation has been encountered in complementary analyses (not included here for the sake of brevity), when soil water profiles assume values that are near to saturation conditions. A closer inspection of the results depicted in Figs. 1 and 2 reveals that an abrupt reduction in soil moisture yields a rapid convergence of n, although it can also induce a failure in the retrieval algorithm. As shown by Vrugt et al. (2001, 2002), most of the information on n is embedded in observations whose pressure heads are located well beyond the inflection point of the soil water retention function. This behaviour is chiefly attributed to the change of the shape of the water capacity function, $C(h)$, and the hydraulic conductivity, $K(h)$, when n changes from $n<2$ to $n>2$ near saturation. As addressed by Vogel et al. (2001), the slopes of these two functions change from $-\infty$ for $C(h)$ and ∞ for $K(h)$ when $n<2$ to some non-zero finite values when $n=2$, and to zero when $n>2$. This can be appreciated in Fig. 3, which shows the hydraulic functions $C(h)$, $K(h)$ and $D(\theta)$ near saturation using the true parameter values as a function of parameter n.

The parameter estimation using the Unscented Kalman Filter, similar to the EKF, can be interpreted as a modified-Newton optimization method, which performs an approximate search over the surface of the squared-prediction-error cost (Nelson, 2000). The anomalies in the concavity of these curves are reflected as changes in the gradient of the cost-function. Romano and Santini (1999) observed that the smaller the values of the retention parameters α and n, the higher the curvature of the response surfaces and thus suggested to choose a first guess vector of the parameters by keeping α and n close to their minimum.

Instead, the identifiability of parameter n in the $\theta-\theta$ retrieving mode has been found always stable, independently from the input value of n. Retrieving θ values instead of h values improves the identifiability of n, at the cost of a light detriment of the identifiability of α. As an opposite trend with respect to the $h-h$ retrieving mode, it is possible to appreciate that the indentifiability with initial $n>2$ improves with respect to that with initial $n<2$ during the initial stage of the simulated process, characterised by high soil water content values.

HESSD
9, 13329–13372, 2012

This result reinforces the feeling that, when n is around 2, the observed convergence patterns are significantly influenced by the shape of $C(h)$, $K(h)$, and (in the θ-based form) their functional ratio $D(\theta)$. Figure 3 also highlights the relative differences between the concavity pattern of the water diffusivity $D(\theta)$ (Fig. 3c) with respect to that of water capacity $C(h)$ and the hydraulic conductivity $K(h)$ (Fig. 3a and b) when parameter n approaches the value of 2. Unlike functions $C(h)$ and $K(h)$, the diffusivity function $D(\theta)$ is not affected by a change of concavity, thus making the convergence in the wet range easier.

Finally, also encouraging is the fact that even for the decreasing resolution of the observations in space and time, the dual approach is able to found a set of parameters that suitably mimics the evolving state profiles. With the aim of illustrating the maximum expected inaccuracy, Fig. 4 depicts the retrieved parameters using the lowest resolution considered, i.e. OD = 2 cm and AF = 1/5 days^{-1}, using both the $h-h$ and the $\theta-\theta$ retrieving modes.

5.3 State retrieving

The results concerning the state identification are also encouraging. Figure 5 shows the retrieved states using the $h-h$ and $\theta-\theta$ retrieving modes after 5, 10, 20, 50, 100 and 150 days, considering the minimum assimilation frequency of near-surface observations (AF = 1/5 days^{-1}). Pressure head profiles corresponding to the initial parameter set S6 are excluded from the results due to persistent failures.

The soil moisture retrieval clearly outperforms the analogous pressure head retrieving using the lowest temporal and spatial resolution of the observations. Nevertheless, as shown later, the average RSME using pressure heads is generally lower. The evolving pressure head profiles S4 and S5 using AF = 1/5 days^{-1} are permanently biased. This result reflects the abnormal pattern of the evolving retrieved parameters associated with these two sets (Fig. 4a), both characterized by an initial guess $n > 2$.

Instead, the performance of the soil moisture retrieving is consistently high with all sets of parameters. At the 50th day, there is already a very good match between the

HESSD
9, 13329–13372, 2012

whole guess profiles and the SD ones, despite the high vertical variability. Figure 5j, showing the temporal evolving of the soil moisture ME and RSME for the entire situations, provides additional insights about the stability and consistency of the θ-form algorithm. Both statistics show a plain trend to zero in all cases. Nevertheless, transient differences are also notable. In particular, it is notable the relatively high ME and RMSE using the lowest assimilation frequencies with respect to daily assimilations.

For better illustrating this statement, Fig. 6 depicts the ratios of the mean RMSE within each group of parameter set computed at the 150th day for different observation depths and assimilation frequencies. The RSME is almost insensitive to increasing observation depths from OD = 2 cm to OD = 5 cm, and just slightly affected by the change from OD = 5 cm to OD = 10 cm (Fig. 7). Whilst, the RMSE by assimilating one observation every three days is approximately twice that corresponding to daily assimilations as average, independently from the observation depths (see Fig. 7b). Instead, the final RSME assimilating every five days is slightly smaller than the RMSE for AF = 1/3 days^{-1}. These trends have been observed also in the h-form, except for the cases with initial sets S4 and S5 using AF = 1/5 days^{-1}, i.e. those affected by anomalies during parameter retrieving.

The ratio of the mean RMSE values computed with the $\theta - \theta$ retrieving mode to those obtained with the $h - h$ mode is about 1.8, roughly independent from all factors examined for the initialization and the implementation of the retrieving algorithm. The convergence of the predicted pressure head profiles to the SD ones is also clearly faster than the predicted soil moisture profiles. This seems to be linked to the higher resolution with which the differences between observations and predictions are represented in the h-form. This could be also due to the not perfect symmetry between the implementation strategies adopted for the retrieving algorithms in the $\theta - \theta$ and in the $h - h$ modes, as for example when assuming a 5 % of the state value as state noise covariance.

Table 3 resumes ME and RMSE values at the 150th day for all examined cases. Blank cells correspond to failed simulations.

HESSD
9, 13329–13372, 2012

5.4 Influence of the type observed variables with respect to the selected state variables

The previous analyses have been focused on the performance involving the $h - h$ and $\theta - \theta$retrieving modes, i.e. when the observed and the retrieved variables are of the same type. This allows for the implementation of a linear observation equation (Eq. 2), with a standard KF for states retrieving. Nevertheless, part of the study has been also focused on the relation between the type of assimilated data and the h-form or θ-form of the state equation.

In principle, the numerical algorithm can be structured to assimilate soil moisture observations (or some information linked to it) in the h-form of the Richard equation, by dealing with a nonlinear observation equation, referred above as the $\theta - h$ retrieving mode. This issue can be frequent, given the structure of many widely used simulation models as well as the type of information provided by current remote sensing techniques and ground-based sensors.

To this point, it is important to note that the inversion of the observation variable, i.e. converting soil moistures to pressure heads by means of a water retention function with guessed (wrong) parameters, would be a severe mistake because the observations would significantly biased, incorporating an unpredictable error in the retrieving algorithm. Differently, a nonlinear relationship for transforming an exogenous observation variable (as for example soil surface temperature from thermal infrared remote sensing) in soil moisture, can be directly employed prior applying the observation operator H in Eq. (2).

The effect of dealing with a nonlinear observation operator within the retrieving algorithm is illustrated in Fig. 8. Figure 8a shows the retrieved parameters using an hourly assimilation frequency, from the $h - h$ retrieving mode. Figure 8b shows the analogous results, but now with the $\theta - h$ retrieving mode, assimilating the equivalent soil moisture observations obtained by simple inversion of the soil water retention curve. In this

HESSD
9, 13329–13372, 2012

case, the unscented algorithm is also employed for the statistical linearization of the now nonlinear operator **H**, similarly to what is done for retrieving the parameters.

Such linearization clearly incorporates a significant amount of errors, which affects sensibly the overall identifiability of the unknown parameters. Note that even the identifiability of parameter α is severely affected by using this strategy. With low assimilation frequencies the algorithm is subjected to the persistent failures.

These results sustain that the state variable and observation variable should be always of the same type, either in the h-form or in θ-form, to avoid the need of linearizing the observation equation (Eq. 2) with respect to the states.

Finally, it is useful to see that in an Extended Kalman filter framework, the non zero elements of the linearized observation operator H would correspond to the hydraulic capacities $C(h)$, evaluated in the prior states values $\hat{\boldsymbol{x}}_k^-$, at the observation nodes. This provides an idea of the unpredictability of the uncertainty attached to the linearization process, as this is strongly influenced by the soil properties.

5.5 Influence of the initial covariance matrices

The dual KF algorithm, as their analogous approaches, requires initial values for the signal-state covariance, $\mathbf{P}_x$, and the weight covariance, $\mathbf{P}_w$. The effect of the initial state covariance matrix $\mathbf{P}_x$, or the noise covariance matrices $\mathbf{R}_v$ and $\mathbf{R}_n$ on the assimilation scheme is straightforward and has been widely examined (see for example Walker, 1999; Nelson, 2000). The reasonable values for the initial parameter covariance $\mathbf{P}_w$ and the artificial noise covariances $\mathbf{R}_r$ and $\mathbf{R}_e$., are less clear and involves several factors (Nelson, 2000).

As stated by Nelson (2000), $\mathbf{R}_e$ acts as a scaling term, determining the relative influence of the initial covariance $\mathbf{P}_{w_0}$ on later covariance matrices $\mathbf{P}_{w_k}$. For a prefixed $\mathbf{P}_{w_0}$, a large $\mathbf{R}_e$ produces more stable (lower variance) behaviour, but this produces significantly biased estimates $\boldsymbol{w}_k$ for small times k. A very small $\mathbf{R}_e$ exposes the algorithm to retrieve parameters toward the corresponding limiting values, mining its stability and

HESSD
9, 13329–13372, 2012

convergence. Notice that this problem is not avoided by simply broaden the allowed parameter range.

An initial value $\mathbf{P}_{w_0} = 10^{-2}$ for the diagonal elements performed well for most of the cases, both with soil moisture and pressure heads as state variables, as found by Nelson (2000) who also employed normalized parameterisation. Once the normalized $\mathbf{P}_w$ is fixed, the value of $\mathbf{R}_e$ strongly depends on the variance of the data, and hence, of the state variable. When retrieving soil moistures, $\mathbf{R}_e$ has been set to 10^{-5}, while when using log-transformed pressure heads, its value has been always tuned according to the specific conditions for avoiding failures, with values ranging from 10^{-5} to 10^{-3}. Nevertheless, using the normal (not log-transformed) *h*-form within our complementary analyses, $\mathbf{R}_e = 0.5$ has been found as appropriate for many applications. In general, the higher the variability of the involved retrieved variable, higher $\mathbf{R}_e$ values are required. In any case, the selection of proper $\mathbf{R}_e$ deserves more attention in further studies, because it seems a determinant stability factor, particularly when using pressure heads.

The prediction error covariance $\mathbf{R}_r$ is also a key variable, having effects in parameter retrieving for longer time intervals. It artificially determines the amount of error incorporated in the parameter covariance matrix, and then it is decisive in convergence and tracking. When comparing the possible options provided by van de Merwe (2004) from Eqs. (21) and (22), only the exponentially decay weighting (by using the "forgetting factor") has been always performing fairly well.

As found by Nelson (2000), a value around $\lambda_{\mathrm{RLS}} = 0.9999$ (see Eq. 30) produces good results using soil moisture and transformed pressure heads. For the standard *h*-form, $\lambda_{\mathrm{RLS}} = 0.995$ is appreciated as a fair value. The Robbins-Monro approach tends to add too noise to the parameter covariance during the synthetic analyses, principally under the *h*-form, even collapsing the simulations. According to Evans et al. (2005), the stochastic gradient algorithms are not scale invariant, and thus the resulting estimates are affected by the units choice.

HESSD
9, 13329–13372, 2012

Ultimately, the choice of a suitable updating strategy is also seen as an important point for future research.

6 Conclusions

Based on the synthetic analyses herein presented, a dual Kalman filter approach seems suitable for simultaneous retrieving of soil moisture (or pressure head) profiles and the soil hydraulic parameters by assimilating near surface soil moisture information. The proposed approach takes the advantages on the linearization of the numerical algorithm of the Richards equation for a straightforward retrieving of the states, and the virtues of the unscented approach for parameter retrieving within a nonlinear framework.

The results demonstrated the efficiency of the unscented approach in linearizing the model with respect to the parameters, without the need to perform any analytical differentiation. This represents a very helpful aspect considering the fact that a transforming equation of unknown parameters could be required between the retrieved parameters and the state space model. The unscented strategy makes the computational implementation very simple and of general applicability, i.e. independent from the analytic equations employed.

The assimilation of near surface soil moisture observations recalls some considerations about the sensitivity to the VGM parameters, at least when the system is initialized with wet conditions. The indentifiability of parameter α is markedly higher than that of n, particularly when using pressure head as retrieving variable. Instead the identifiability of the saturated hydraulic conductivity is in all cases very poor. This fact, joined with the strong correlation observed between retrieved n and K_s, suggests the opportunity to employ other analytical models, representing the hydraulic conductivity decoupled from the retention function.

An encouraging finding is that the dual Kalman Filter approach is able to find a parametric solution while retrieving states closed to the true values, even for lightest

HESSD
9, 13329–13372, 2012

near-surface observations, i.e. using observation depths of 2 cm and assimilation frequency of one every five days. The comparison between parameter initialization, observation depth and assimilation frequency evidenced that the latter has the most dominant effect on the evolving errors. The temporal patterns of ME and RMSE values are in particular sensitive to the assimilation frequency, with increasing values from daily to once every three days.

The problem associated to adopting either the h-form or θ-form of the Richards equation in the dual Kalman Filter algorithm has been explored. A fundamental drawback associated with retrieving pressure heads is the low algorithm stability, being highly vulnerable to several physical and mathematical issues. Whilst, the θ-form is appreciated as very stable and efficient to deal with unsaturated conditions within the dual retrieving process. Nevertheless, being stable, the pressure heads retrieving algorithm outperformed that using soil moisture in terms of state convergence and final accuracy.

Finally, by examining different combinations of retrieved and assimilated variables, the study definitively demonstrates the several edges behind the efficiency of the dual Kalman Filter approach, beside the Kalman Filter extension per se. The present study sustains the convenience of retrieving state variable of the same type of the observation variable, as this permits to employ a linear observation equation. The performance of the overall retrieving process is significantly dampened when using an algorithm based on the assimilation of soil moisture as observation variable and pressure head as the retrieving variable, even with observations assimilated hourly.

Acknowledgements. This study has been supported by P.O.N. project "AQUATEC – New technologies of control, treatment, and maintenance for the solution of water emergency". Hanoi Medina has been also supported by the Abdus Salam International Centre for Theoretical Physics (ICTP), where he has been appointed as Junior Associate.

HESSD
9, 13329–13372, 2012

References

Calvet, J. C. and Noilhan, J.: From near-surface to root-zone soil moisture using year-round data, J. Hydrometeorol., 1, 393–411, 2000.

Chirico, G. B., Medina, H., and Romano, N.: Uncertainty in predicting soil hydraulic properties at the hillslope scale with indirect methods, J. Hydrol., 334, 405–422, 2007.

Chirico, G. B., Medina, H., and Romano, N.: Functional evaluation of PTF prediction uncertainty: an application at hillslope scale, Geoderma, 155, 193–202, 2010.

Chirico, G. B., Medina, H., and Romano, N.: Kalman filters for assimilating near-surface observations in the Richards equation – Part 1: Retrieving state profiles with linear and nonlinear numerical schemes, Hydrol. Earth Syst. Sci. Discuss., 9, 13291–13327, doi:10.5194/hessd-9-13291-2012, 2012.

Crow, W. T. and Wood, E. F.: The assimilation of remotely sensed soil brightness temperature imagery into a land surface model using ensemble Kalman filtering: A case study based on ESTAR measurements during SGP97, Adv. Water Resour., 26, 137–149, 2003.

Das, N. N. and Mohanty, B. P.: Root zone soil moisture assessment using remote sensing and vadose zone modeling, Vadose Zone J., 5, 296–307, 2006.

De Lannoy, G. J. M., Reichle, R. H., Houser, P. R., Pauwels, V. R. N., and Verhoest, N. E. C.: Correcting for forecast bias in soil moisture assimilation with the ensemble Kalman filter, Water Resour. Res., 43, W09410, doi:10.1029/2006WR005449, 2007.

Entekhabi, D., Nakamura, H., and Njoku, E. G.: Solving the inverse problem for soil moisture and temperature profiles by sequential assimilation of multifrecuency remote sensed observations, IEEE T. Geosci. Remote, 32, 438–448, 1994.

Escorihuela, M. J., Chanzy, A., Wigneron, J. P., and Kerr, Y. H.: Effective soil moisture sampling depth of L-band radiometry: A case study, Remote Sens. Environ., 114, 995–1001, 2010.

Evans, G. W., Honkapohja, S., and Williams, N.: Generalized Stochastic Gradient Learning, Cambridge Working Papers in Economics 0545, Faculty of Economics, University of Cambridge, 2005.

Gove, J. H. and Hollinger, D. Y.: Application of a dual unscented Kalman filter for simultaneous state and parameter estimation in problems of surface-atmosphere exchange, J. Geophys. Res.-Atmos., 111, D08S07, doi:10.1029/2005JD006021, 2006.

Heathman, G. C., Starks, P. J., Ahuja, L. R., and Jackson, T. J.: Assimilation of surface soil moisture to estimate profile soil water content, J. Hydrol., 279, 1–17, 2003.

HESSD
9, 13329–13372, 2012

Julier, S. J. and Uhlmann, J. K.: A New Extension of the Kalman Filter to Nonlinear Systems, Proc. SPIE, 3068, 182–193, 1997.
Julier, S. J., Uhlmann, J. K., and Durrant-Whyte, H. F.: A new approach for filtering nonlinear systems, in: The Proceedings of the American Control Conference, Seattle WA, USA, 1628–1632, 1995.
Jury, W. A., Gardner, W. R., and Gardner, W. H.: Soil Physics, 5th Edn., John Wiley, New York, 1991.
Kalman, R. E.: A New Approach to Linear Filtering and Prediction Problems, ASME J. Basic Eng., 82D, 35–45, 1960.
Kerr, Y. H.: Soil moisture from space. Where are we?, Hydrogeol. J., 15, 117–120, 2007.
Li, F. Q., Crow, W. T., and Kustas, W. P.: Towards the estimation root-zone soil moisture via the simultaneous assimilation of thermal and microwave soil moisture retrievals, Adv. Water Resour., 33, 201–214, 2010.
McLaughlin, D. B.: An integrated approach to hydrologic data assimilation: Interpolation, smoothing, and filtering, Adv. Water Resour., 25, 1275–1286, 2002.
Medina, H., Romano, N., and Chirico, G. B.: Kalman filters for assimilating near-surface observations in the Richards equation – Part 3: Retrieving states and parameters from laboratory evaporation experiments, Hydrol. Earth Syst. Sci. Discuss., 9, 13373–13414, doi:10.5194/hessd-9-13373-2012, 2012.
Montzka, C., Moradkhani, H., Weihermuller, L., Hendricks-Franssen, H. J., Canty, M., and Vereecken, H.: Hydraulic parameter estimation by remotely-sensed top soil moisture observations with the particle filter, J. Hydrol., 399, 410–421, 2011.
Moradkhani, H., Sorooshian, S., Gupta, H. V., and Houser, P.: Dual state-parameter estimation of hydrological models using Ensemble Kalman filter, Adv. Water Resour., 28, 135–147, 2005.
Nasta, P., Kamai, T., Chirico, G. B., Hopmans, J. W., and Romano, N.: Scaling soil water retention functions using particle-size distribution, J. Hydrol., 374, 223–234, 2009.
Nelson, A. T.: Nonlinear estimation and modeling of noisy time-series by dual Kalman filter methods, PhD thesis, Oregon Graduate Institute of Science and Technology, 281 pp., 2000.
Press, W. H., Teukolsky, S. A., Vetterling, W. T., and Flannery, B. P.: Numerical Recipes in C: The Art of Scientific Computing, 2nd Edn., Cambridge University Press, 1992.
Pringle, M. J., Romano, N., Minasny, B., Chirico, G. B., and Lark, R. M.: Spatial evaluation of pedotransfer functions using wavelet analysis, J. Hydrol., 333, 182–198, 2007.

HESSD
9, 13329–13372, 2012

Qin, J., Liang, S. L., Yang, K., Kaihotsu, I., Liu, R. G., and Koike, T.: Simultaneous estimation of both soil moisture and model parameters using particle filtering method through the assimilation of microwave signal, J. Geophys. Res.-Atmos., 114, D15103, doi:10.1029/2008JD011358, 2009.

Ritter, A., Muñoz-Carpena, R., Regalado, C. M., Vanclooster, M., and Lambot, S.: Analysis of alternative measurement strategies for the inverse optimization of the hydraulic properties of a volcanic soil, J. Hydrol., 295, 124–139, 2004.

Romano, N. and Santini, A.: Determining soil hydraulic functions from evaporation experiments by a parameter estimation approach: Experimental verifications and numerical studies, Water Resour. Res., 35, 3343–3359, 1999.

Scharnagl, B., Vrugt, J. A., Vereecken, H., and Herbst, M.: Inverse modelling of in situ soil water dynamics: investigating the effect of different prior distributions of the soil hydraulic parameters, Hydrol. Earth Syst. Sci., 15, 3043–3059, doi:10.5194/hess-15-3043-2011, 2011.

Tian, X., Xie, Z., and Dai, A.: A land surface soil moisture data assimilation system based on the dual-UKF method and the Community Land Model, J. Geophys. Res., 113, D14127, doi:10.1029/2007JD009650, 2008.

van der Merwe, R.: Sigma-Point Kalman Filters for Probabilistic Inference in Dynamic State-Space Models, PhD dissertation, University of Washington, USA, 2004.

van Genuchten, M. Th.: A closed-form equation for predicting the hydraulic conductivity of unsaturated soils, Soil Sci. Soc. Am. J., 44, 892–898, 1980.

Qin, J., Liang, S. L., Yang, K., Kaihotsu, I., Liu, R. G., and Koike, T.: Simultaneous estimation of both soil moisture and model parameters using particle filtering method through the assimilation of microwave signal, J. Geophys. Res.-Atmos., 114, D15103, doi:10.1029/2008JD011358, 2009.

Vogel, T., van Genuchten, M. T., and Cislerova, M.: Effect of the shape of soil hydraulic functions near saturation on variably-saturated flow predictions, Adv. Water Resour., 24, 133–144, 2001.

Vrugt, J. A., Bouten, W., and Weerts, A. H.: Information content of data for identifying soil hydraulic parameters from outflow experiments, Soil Sci. Soc. Am. J., 65, 19–27, 2001.

Vrugt, J. A., Bouten, W., Gupta, H. V., and Sorooshian, S.: Toward improved identifiability of hydrologic model parameters: the information content of experimental data, Water Resour. Res., 38, 1312, doi:10.1029/2001WR001118, 2002.

HESSD
9, 13329–13372, 2012

Walker, J. P.: Estimating soil moisture pro?le dynamics from near-surface soil moisture measurements and standard meteorological data, Ph.D. thesis, The University of Newcastle, Callaghan, New South Wales, Australia, 766 pp., 1999.

Walker, J. P., Willgoose, G. R., and Kalma, J. D.: One-dimensional soil moisture profile retrieval by assimilation of near-surface observations: a comparison of retrieval algorithms, Adv. Water Resour., 24, 631–650, 2001.

Walker, J. P., Houser, P. R., and Willgoose, G. R.: Active microwave remote sensing for soil moisture measurement: a field evaluation using ERS-2, Hydrol. Process., 18 , 1975–1997, 2004.

Wan, E. A. and Nelson, A. T.: Neural Dual Extended Kalman Filtering: Applications in Speech Enhancement and Monaural Blind Signal Separation, in: Proceedings of the IEEE Signal Processing Society Neural Networks for Signal Processing Workshop, New York, 466–475, 1997.

Yang, K., Koike, T., Kaihotsu, I., and Qin, J.: Validation of a dual-pass microwave land data assimilation system for estimating surface soil moisture in semiarid regions, J. Hydrometeorol., 10, 780–793, 2009.

Zhu, J. and Mohanty, B. P.: Soil hydraulic parameter upscaling for steady flow with root water uptake, Vadose Zone J., 3, 1464–1470, 2004.

HESSD

9, 13329–13372, 2012

Table 1. Main parameters and initial conditions employed in the retrieving algorithm.

Input variable	Synthetic data (SD)	
	Pressure head retrieving	Soil moisture retrieving
Initial state variable	−100 cm	0.47 cm^3 cm^{-3*}
Observation depths (OD)	2, 5 and 10 cm	2, 5, 10 cm
Assimilation frequency (AF)	Every 1 and 5 days	Every 1 and 5 days
Initial state covariance matrix $\mathbf{P}^{x}_{i,i}$; $i = 1 \ldots N_{\text{nod}}$	10^3 cm^2	0.8 cm^6 cm^{-6*}
Initial normalized correction terms matrix $\mathbf{P}^{w}_{i,i}$; $i = 1 \ldots N_{\text{par}}$	0.01	0.01
Process-noise updating $\mathbf{R}_{v_{i,i}}$; $i = 1 \ldots N_{\text{nod}}$	0.05 $\boldsymbol{x}_i$ cm^2	0.05 $\boldsymbol{x}_i$ cm^6 cm^{-6}
Observation noise updating $\mathbf{R}_{n_{i,i}}$; $i = 1 \ldots N_{\text{obs}}$	0.02 $\boldsymbol{y}_i$ cm^2	0.02 $\boldsymbol{y}_i$ cm^6 cm^{-6}

N_{nod} is the number of nodes (states); N_{par} is the number of parameters under scrutiny; N_{obs}, is the number of observations; $\boldsymbol{x}$ and $\boldsymbol{y}$ represent the state and the observation vectors, respectively. * Obtained by transforming the corresponding pressure head condition by means of the true soil water retention function.

HESSD
9, 13329–13372, 2012

Table 2. Values of w_{min} and $w_{max} - w_{min}$, used to constrain the distribution of the parameters *Ks*, α and n, and the resulting six sets of input values considered during the assimilation process.

Parameter	w_{min}	$w_{max} - w_{min}$	S1	S2	S3	S4	S5	S6
Ks ($cm\,s^{-1}$)	1×10^{-5}	6×10^{-4}	4.6×10^{-4}	4.6×10^{-4}	3.1×10^{-4}	3.1×10^{-4}	1.6×10^{-4}	1.6×10^{-4}
α (cm^{-1})	1×10^{-3}	5×10^{-2}	2.6×10^{-2}	1.35×10^{-2}	3.85×10^{-2}	1.35×10^{-2}	2.6×10^{-2}	3.85×10^{-2}
n (–)	1.1	2.0	1.6	2.1	1.6	2.6	2.6	2.1

HESSD
9, 13329–13372, 2012

Table 3. Mean error (ME) and RMSE (RMSE) between retrieved pressure head and soil moisture profiles and the true ones, involving the six sets of initial parameters (S1-S6), the three observation depths, (OD = 2, 5 and 10 cm) and the three assimilation frequencies (AF = 1 day^{-1}, 1/3 days^{-1} and 1/5 days^{-1}).

		Retrieving pressure heads						Retrieving soil moistures					
		OD = 2 cm		OD = 5 cm		OD = 10 cm		OD = 2 cm		OD = 5cm		OD = 10cm	
AF	Set	ME	RMSE	ME	RMSE	ME	RMSE	ME	RMSE	ME	RMSE	ME	RMSE
1 day^{-1}	S1	0.0168	0.0312	0.0397	0.0488	0.0493	0.0569	0.0138	0.0232	0.0123	0.0171	0.0076	0.0131
	S2	0.0064	0.0154	0.0268	0.0314	0.0359	0.0424	−0.0920	0.1003	−0.0921	0.1072	−0.0587	0.0787
	S3							0.0560	0.0681	0.0412	0.0481	0.0225	0.0269
	S4	−0.0051	0.0098	−0.0271	0.0632	−0.0221	0.0599	0.0050	0.0190	0.0312	0.0387	0.0440	0.0539
	S5	−0.0230	0.0591	−0.0242	0.0376	0.0136	0.0192	0.0831	0.0922	0.0773	0.0863	0.0560	0.0664
	S6	0.0606	0.1046					0.0556	0.0653	0.0402	0.0459	0.0220	0.0270
1/3 day^{-1}	S1	0.0538	0.0655	0.0539	0.0663	0.0595	0.0719	0.0547	0.0706	0.0388	0.0499	0.0216	0.0289
	S2	0.0396	0.0466	0.0339	0.0400	0.0366	0.0438	−0.0465	0.0788	−0.0551	0.0979	−0.0342	0.0870
	S3	0.0656	0.0818	0.0622	0.0776	0.0649	0.0795	0.1044	0.1376	0.0773	0.1043	0.0491	0.0743
	S4	0.0502	0.0622	0.0776	0.1755	−0.1056	0.1749	0.0222	0.0333	0.0399	0.0639	0.0316	0.0941
	S5	−0.0019	0.0181	0.0600	0.0772	0.0354	0.0424	0.0910	0.1617	0.0752	0.1682	0.0420	0.1567
	S6					0.0575	0.0690	0.1073	0.1391	0.0908	0.1214	0.0650	0.1005
1/5 day^{-1}	S1	0.0334	0.0399	0.0256	0.0299	0.0179	0.0237	0.0201	0.0244	0.0199	0.0228	0.0156	0.0200
	S2	0.0215	0.0308	0.0181	0.0312	0.0095	0.0261	0.0251	0.0724	0.0024	0.1072	−0.0029	0.1279
	S3	0.0342	0.0499	0.0286	0.0347	0.0177	0.0235	−0.0004	0.0817	0.0020	0.0750	−0.0030	0.0684
	S4	−0.4244	0.4443	−0.3199	0.3459			−0.0062	0.0331	−0.0187	0.0541	−0.0568	0.1097
	S5	−0.2332	0.2595	−0.4683	0.4909	−0.1976	0.2424	−0.0698	0.1483	−0.0905	0.1733	−0.0963	0.1900
	S6							−0.0109	0.0922	−0.0016	0.0812	−0.0089	0.0950

HESSD
9, 13329–13372, 2012

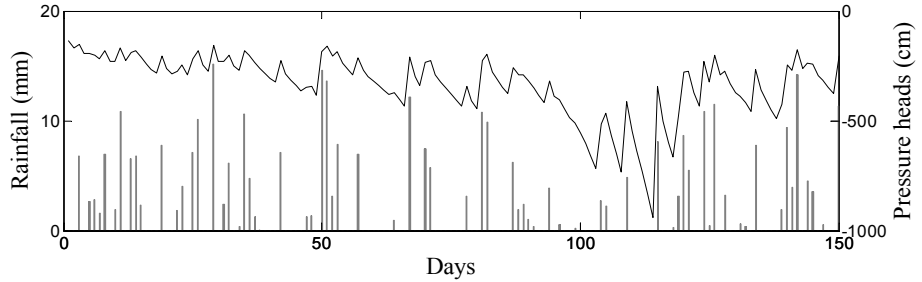

Fig. 1. Rainfall pattern (bar plot) and synthetically generated "true" pressure head values at 5 cm depth (solid line).

HESSD
9, 13329–13372, 2012

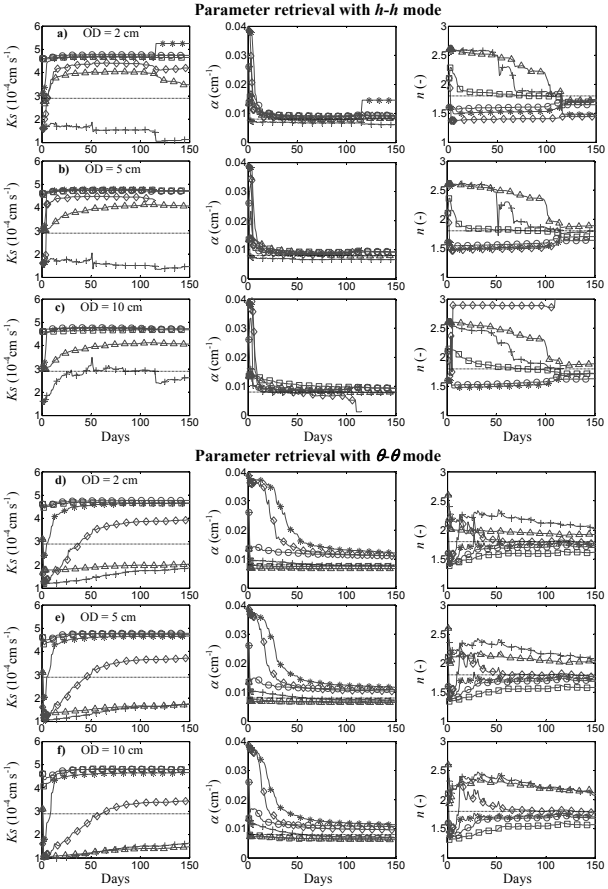

Fig. 2. Retrieved VGM parameters *Ks*, α and *n* using the $h - h$ **(a)–(c)** and the $\theta - \theta$ **(d)–(f)** retrieving modes, with assimilation frequency AF = 1 days^{-1} and observation depth (OD): **(a, d)** 2 cm; **(b, e)** 5 cm; **(c, f)** 10 cm. Comparisons account for the six pondered sets of initial parameters: S1(○), S2(□), S3(∗), S4(Δ), S5(+) and S6(◊). The dotted line indicates the true value.

HESSD
9, 13329–13372, 2012

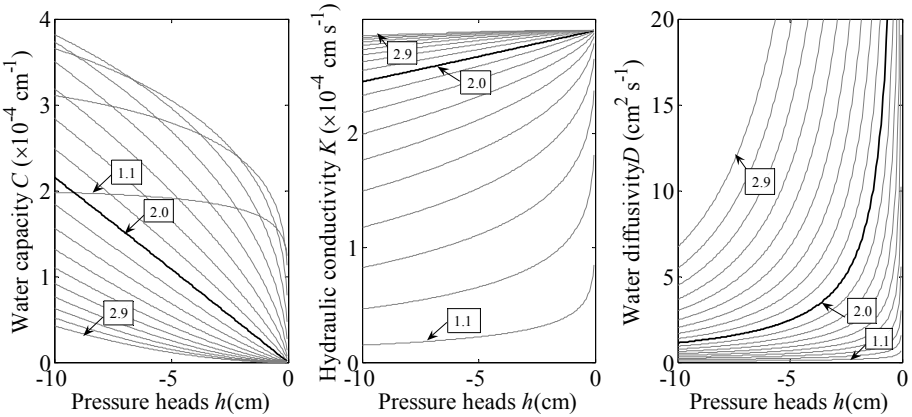

Fig. 3. Plots of the hydraulic capacity $C(h)$, the hydraulic conductivity, $K(h)$ and the hydraulic diffusivity, $D(\theta)$, near saturation using the true parameter values as a function of the parameter n.

HESSD
9, 13329–13372, 2012

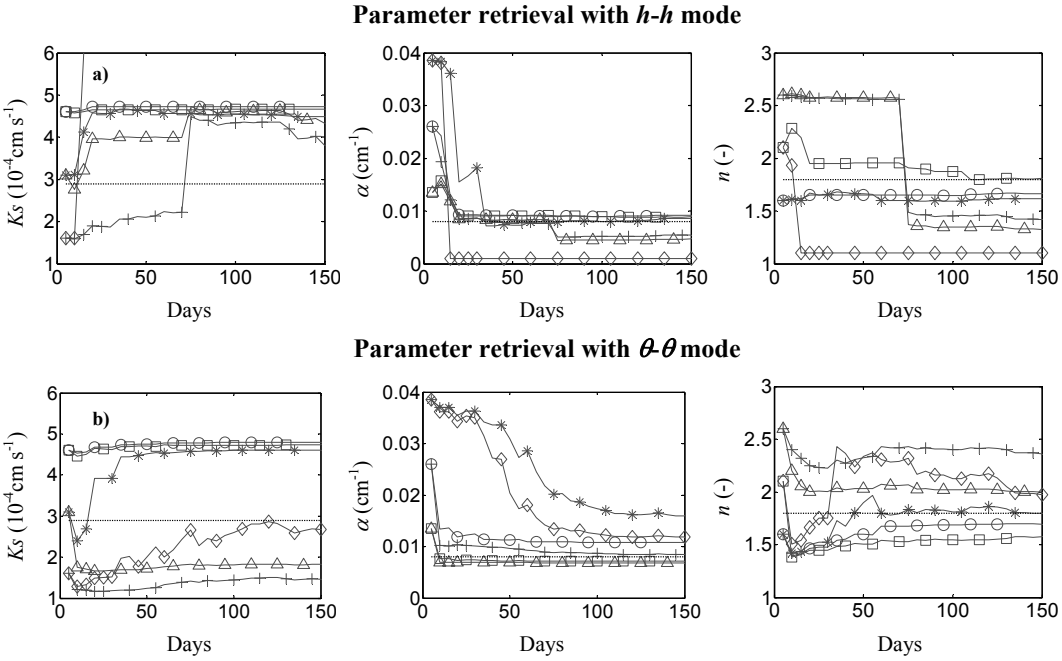

Fig. 4. Retrieved VGM parameters, *Ks*, α and n using **(a)** the $h - h$ and **(b)** the $\theta - \theta$ retrieving modes, with assimilation frequency AF = 1/5 days^{-1} and observation depth OD = 2 cm. Comparisons account for the six pondered sets of initial parameters: S1(◯), S2(□), S3(∗), S4(Δ), S5(+) and S6(◊). The dotted line indicates the true value.

HESSD
9, 13329–13372, 2012

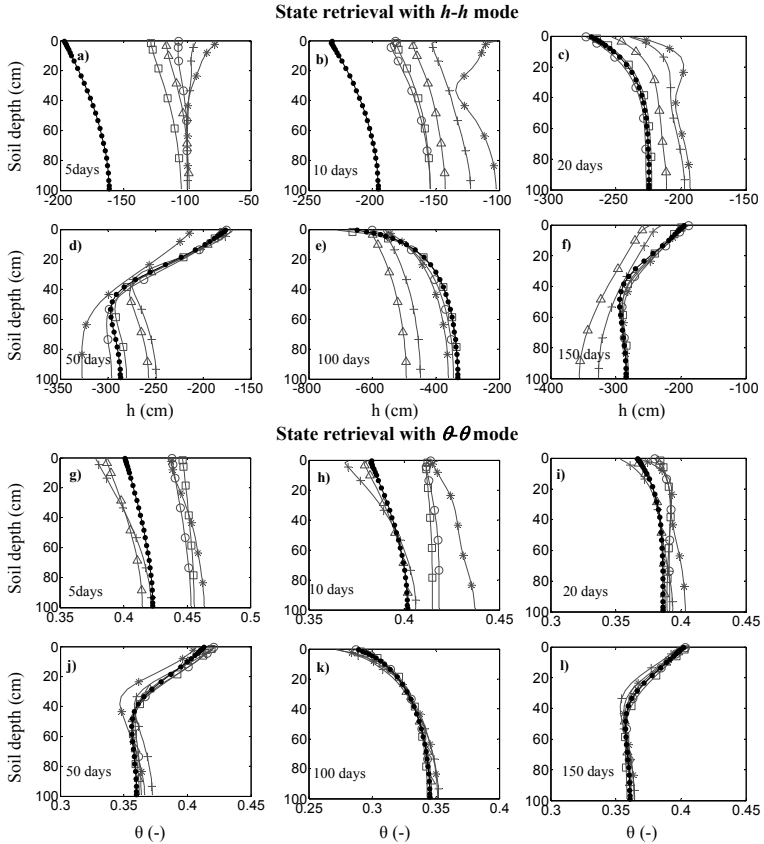

Fig. 5. Retrieved states using the $h - h$ **(a)–(f)** and $\theta - \theta$ **(g)–(l)** modes after 5 **(a, g)**; 10 **(b, h)**; 20 **(c, i)**; 50 **(d, j)**; 100 **(e, k)** and 150 **(f, l)** days, with assimilation frequency AF = 1 days^{-1} and observation depth OD = 2 cm. Comparisons account for the six pondered sets of initial parameters: S1(◯), S2(□), S3(∗), S4(Δ), S5(+) and S6(◊). The dotted line with solid circles represents the true profile.

HESSD
9, 13329–13372, 2012

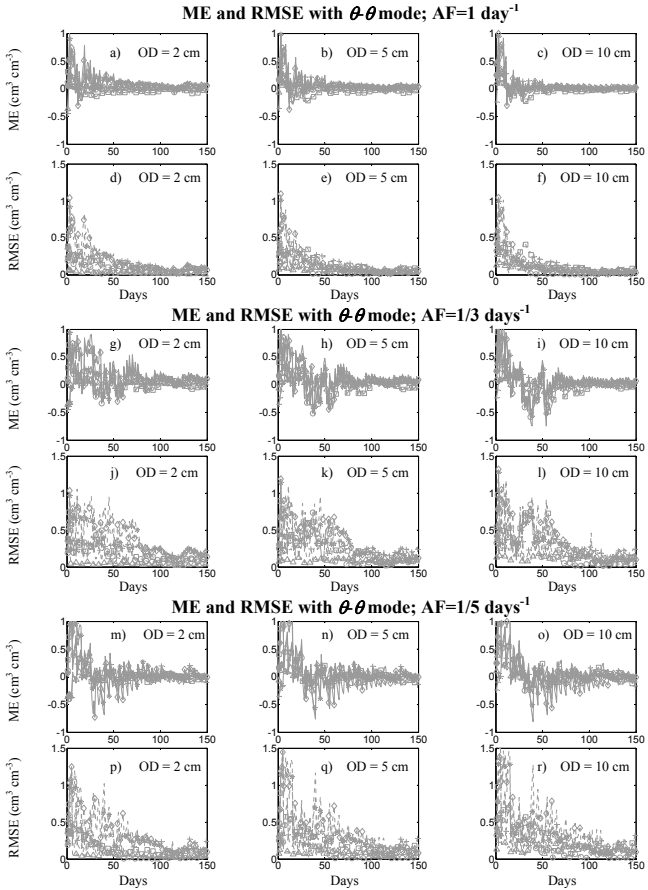

Fig. 6. Normalized mean error (ME) and root mean square error (RMSE) between guess and true soil moisture profiles using the $\theta - \theta$ mode. Assimilation frequency AF – days^{-1}): **(a)–(f)** 1; **(g)–(l)** 1/3 and **(m)–(r)** 1/5. Observation depth (OD): 2 cm (left column), 5 cm (central column) and 10 cm (right column). Comparisons account for the six pondered sets of initial parameters: S1(◯), S2(□), S3(∗), S4(Δ), S5(+) and S6(◊).

HESSD
9, 13329–13372, 2012

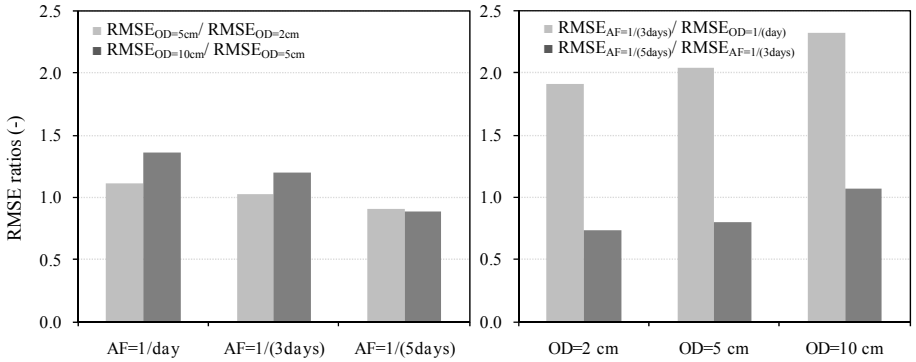

Fig. 7. Ensemble (involving the six parametric sets) of soil moisture RMSE ratios between contiguously sampled **(a)** observation nodes (OD) and **(b)** assimilation frequencies (AF).

HESSD
9, 13329–13372, 2012

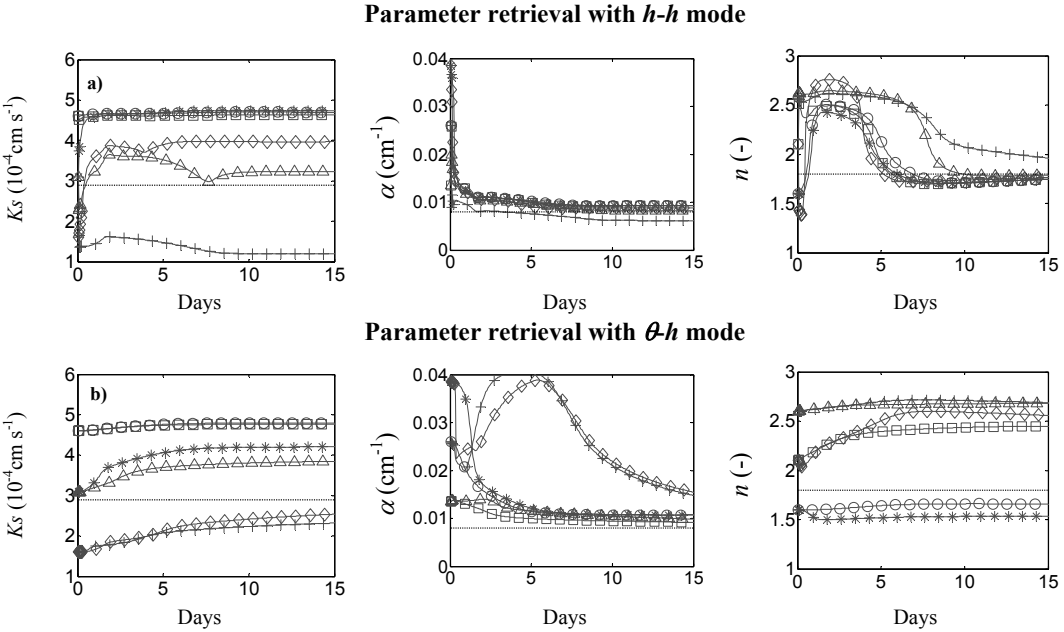

Fig. 8. Retrieved VGM parameters *Ks*, α and *n*, using **(a)** the $h-h$ and **(b)** $\theta-h$ retrieving modes by assimilating observations every hour, with observation depth OD = 10 cm. Comparisons account for the six pondered sets of initial parameters: S1(◯), S2(□), S3(∗), S4(Δ), S5(+) and S6(◊).

HESSD
9, 13329–13372, 2012